Alexandria Engineering Journal (2022) 61, 5097–5109

HOSTED BY
ELSEVIER

Alexandria University
Alexandria Engineering Journal
www.elsevier.com/locate/aej
www.sciencedirect.com

Energetic assessment of a precalcining rotary kiln in a cement plant using process simulator and neural networks

Anthony I. Okoji[a,b,c,d,*], **Ambrose N. Anozie**[c], **James A. Omoleye**[c], **Abiola E. Taiwo**[a,d], **Funmilayo N. Osuolale**[e]

[a] *Landmark University SDG 7 (Affordable and Clean Energy Research Group), Nigeria*
[b] *Landmark University SDG 9 (Industry, Innovation and Infrastructure Research Group), Nigeria*
[c] *Department of Chemical Engineering, Covenant University, Ota, Ogun State, Nigeria*
[d] *Department of Chemical Engineering, Landmark University, Omu-Aran, Kwara State, Nigeria*
[e] *Department of Chemical Engineering, Ladoke Akintola University of Technology, Ogbomoso, Oyo State, Nigeria*

Received 12 May 2021; revised 8 September 2021; accepted 4 October 2021
Available online 14 November 2021

KEYWORDS

Energy efficiency;
Precalcining kiln;
Cement production;
Artificial neural network (ANN);
Bootstrap aggregated neural network (BANN)

Abstract Cement production has been increasing rapidly leading to energy consumption, with serious cost implications and environmental challenges. Energy efficiency is a key component required to maintain the cement company's environmental strategy. In this study, Aspen Plus process model and neural networks are used to assess the energetic efficiency of a precalcining rotary kiln in a cement production process. Aspen Plus process simulator estimated energy efficiency at 61.30 % using the first law of thermodynamic. Further, for the ANN model, kiln feed, kiln gas, calciner gas, clinker cooling air, and primary air were the operation parameters inputs. ANN model is validated and demonstrated it is capable of predicting cement rotary kiln energy efficiency accurately with a correlation coefficient (R^2) of 0.991. In conclusion, the Bootstrap aggregated neural network (BANN) was used to search the optimal operational parameters in achieving the lowest mean square error (MSE) of the energy efficiency. The MSE for training, testing, and validation data sets were 3.64×10^{-5}, 3.70×10^{-5}, and 5.00×10^{-5} for in the estimation of rotary kiln system energy efficiency. To achieve this optimal condition of 61.5 % energy efficiency, the optimal parameters as determined by ANN (BANN) were kiln feed of 205050 kg/hr, kiln fuel gas of 2821 kg/hr, calciner fuel gas of 5648 kg/hr, clinker cooling air of 247463 kg/hr and primary air of 7309 kg/hr. Consequently, it is recommended that ANN should be combined with Bootstrap aggregated neural network (BANN) for effective prediction and monitoring of energy efficiency for precalcining rotary kiln system.

* Corresponding author at: Department of Chemical Engineering, Landmark University, Omu-Aran, Kwara state, Nigeria.
E-mail address: okoji.anthony@lmu.edu.ng (A.I. Okoji).

Peer review under responsibility of Faculty of Engineering, Alexandria University.

https://doi.org/10.1016/j.aej.2021.10.010
1110-0168

1. Introduction

Cement demand in high quantity was initiated by the global rapid urbanization. Global cement as of 2019 was projected to be 5.2 billion metric tons and half of the figures were accrued to Asia/Pacific region being the world's largest consumer. A developing country like Nigeria has shown a corresponding increase in demand for raw materials and energy due to considerable evolution in its production capacity of cement [1]. This necessitates the need for energy evaluation of the cement industry for both thermal and electrical energy. Cement rotary kiln is the main equipment commonly used in the modern cement industry to manufacture cement clinker. Hence, it becomes essential to study the energy efficiency in a cement rotary kiln that will satisfy the design and optimization of the cement manufacturing process.

Several studies addressing the cement industry's energetic efficiency have increased significantly with a focus on thermal energy reduction. Worrell and Reuter [2] examined over 50 energy-efficient technologies and initiatives. These authors projected energy reductions, reductions in carbon dioxide emissions, investment costs, operational and maintenance costs were analyzed for each of the initiatives. Utlu *et al.,* [3] study on the raw mill sub-system reported that the energy efficiency of the cement was 84.3% but without consideration of the precalcining rotary kiln. Fellaou and Bounahmidi [4] examined the energy efficiency opportunities of a typical Moroccan cement plant. Energy analysis tool was used by different authors to examined the cement plant precalcining rotary kiln unit [5–7]. Cement plant pyroprocessing unit using an energy analysis tool had been studied in different research works [8–11]. Talaei *et al.,* [12] develop a technological framework and energy model in the cement industry with a focus on energy savings in the cement sector.

However, the authors did not use a process simulator in the estimation of the energy assessment. Therefore, due to the complexity involved in the mass and energy balance; the in-line precalciner rotary kiln units pose a great challenge for the plant operators to control. Past studies have reported the use of software based on computational fluid dynamics (CFD) to primarily model the process's rotary kiln segment [13–14]. Basically, a one-dimensional balance for energy and material was used that is capable of handling the solid particle's behavior in a standard CFD environment [15–16]. Mechanistic models have been used for studies on energy efficiency. However, it may be complicated and time-consuming to develop such a model for complex processes particularly to integrate energy efficiency in the second law of thermodynamics [17]. Data-based models such as Aspen Plus [18], artificial neural network (ANN) and bootstrap aggregated neural network (BANN) models could help resolve these issues [19–21].

An ANN is a field of artificial intelligence that is capable of identifying non-linear relationships between inputs and outputs of a system. An artificial neural network (ANN), which uses machine-learning to build non-statistical models, functions similarly to the human brain in distributed parallel processing [10]. It is evident that the ANN enables diagnoses, improves control with accuracy and flexibility of forecasting with data training of the system's performance [11].

Artificial Neural network (ANN) has proven capable of approximating continuous non-linear functions. ANN helps in solving complex nonlinear problems and for applications in automation control, prediction in bioreactor, haloketones prediction in tap water, pattern recognition, signal processing prediction, modeling, optimization [22–26]. ANN has been successfully used in many predictive modeling and optimization problems, including enzyme production optimization [27], biogas production prediction [28] and air pollutant prediction [29]. By implementing a polynomial neural network in cement plants, Koumboulis and Kouvakas [30] were able to control the abgasses temperature as well as achieving a desired precalcination level. Marengo *et al.,* [31] examined the modeling of pollution emissions from a cement production plant using PCRegression, partial least-squares, and artificial neural networks. The results of the study concluded that ANNs are significantly more effective than PLS and PCR in prediction and are comparable to experimental uncertainty of the response, at least for SO_2 and dust. Developing a number of neural network models and combining them is an attractive method of improving neural network model robustness.

A stacked or bootstrap neural network is such a combination of two or more individual neural networks [32–34] that makes predictions based on the combined predictions of each neural network. Zhang [21] used bootstrap aggregated neural networks in building of software sensors for a batch polymerisation reactor. It was shown that the models was more accurate and robust than those built from single neural networks. Osuolale and Zhang [19], have reported that bootstrap aggregated neural network (BANN) is a good search engine for determining optimal operational parameters in achieving the lowest mean square error (MSE) of the energy efficiency in a process plant.

Consequently, this paper is aimed at predicting energy efficiency of a precalcining rotary kiln of a cement plant using artificial neural networks (ANN). Although, ANN has been employed in evaluating other processes, however, to the best of our knowledge, this is the first study that would assimilate artificial neural network model with Bootstrap aggregated neural networks to improve the prediction and monitoring of the energy efficiency of a precalcining rotary kiln.

2. Cement production process description

The production of cement is sub-divided into two processes: first "clinker" is produced at a temperature of 1450 °C and secondly, the clinker is ground to the powder known as cement with other minerals. Fig. 1 below shows a process flowchart of a dry cement manufacturing technology. The process simulator using Aspen Plus is described in detail below and represented using a process flow sheet in Fig. 2.

2.1. Cyclone

The kiln feed material, one of the operation parameters was introduced into the process through the topmost preheater cyclone, and this is to assist in raw material 'preheat' within the tower. The preheating tower was simulated as a series of mixers and cyclones in Fig. 2. The solid (kiln feed-raw meal) mixed with the gas flow below in each mixer; assumed heat exchange in the process. The mixture was sent to a cyclone and separated. The temperatures of the gas and solids assumed the same in each cyclone stage. The efficiency of each cyclone is

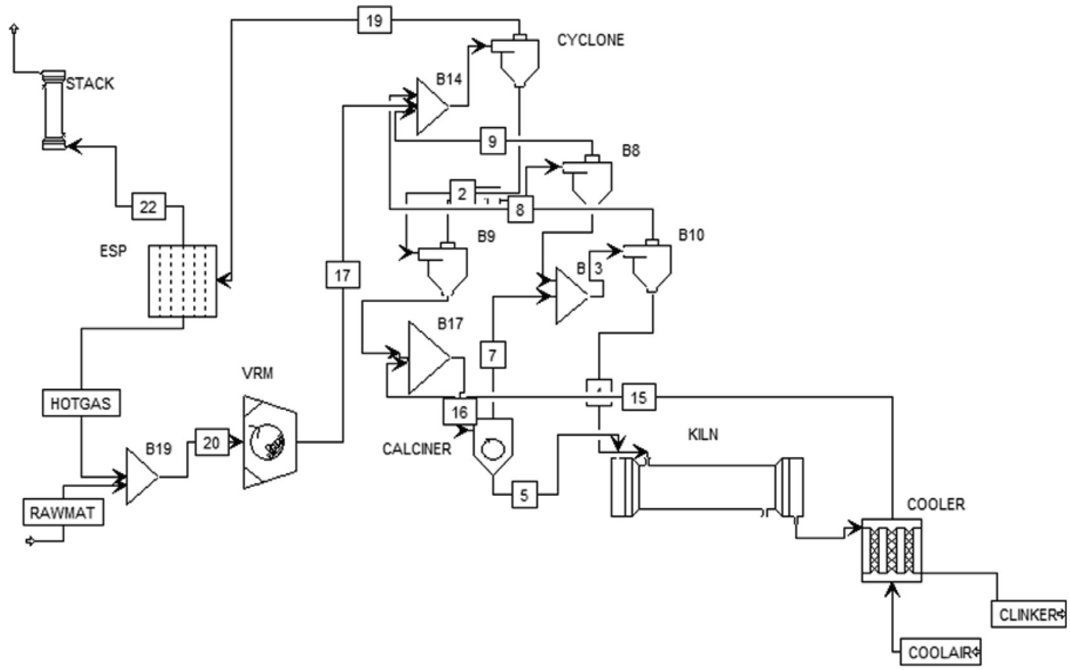

Fig. 1 Schematic layout of a typical cement plant.

set to reflect the dust emission of the reference cement plant studied. The separated (preheated) material dropped to the calciner vessel by gravity.

2.2. Calciner

The calciner gas being an operation parameter was introduced, and mixed with the combustion air from the clinker cooler through both the tertiary and secondary air ducts for calcination process to be effective. The calcination process is a chemical reaction and is represented in a simulator in two steps. The calciner process consists of the following sections in Fig. 2: Separator (Cyclone), Combustor (COMBUST), Calciner (RStoic). The calciner is where the calcination takes place and the heat for the process is supplied from the combustor using natural gas as the main fuel. The combustion occurs in

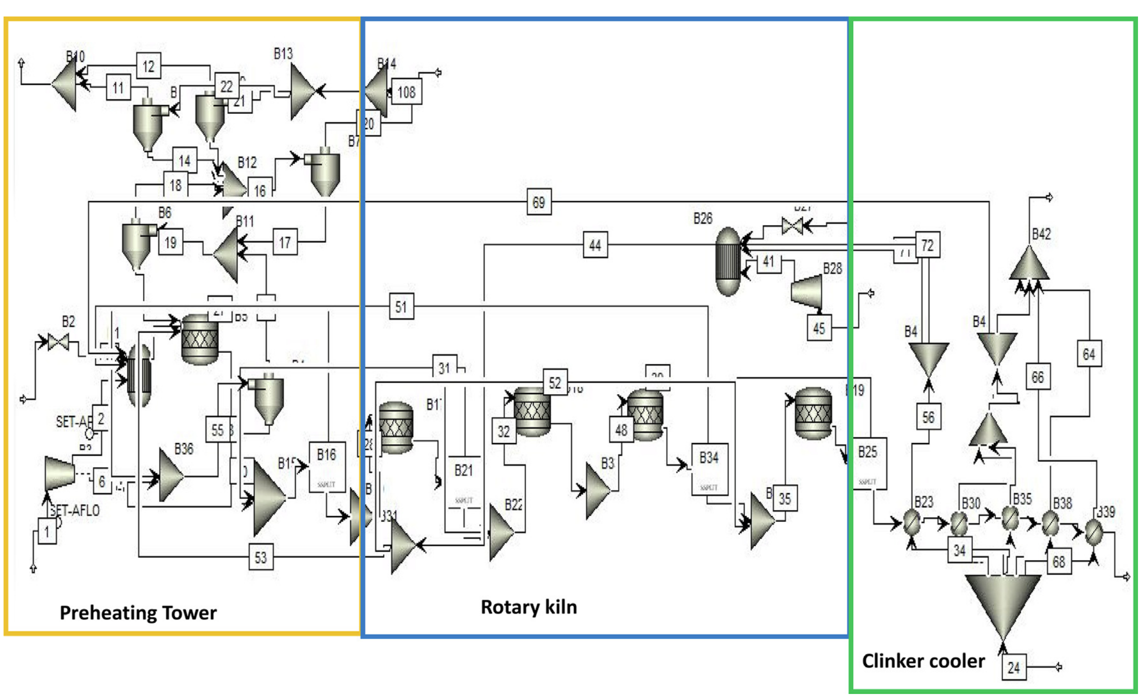

Fig. 2 Aspen Plus process simulator flow sheet for a typical cement manufacturing.

combustor (RGIBBS reactor) while calcination takes place in Calcinator (RStoic reactor) of Aspen Plus simulator. These are endothermal reactions and the heat provided by the flue gases of natural gas combustion from the combustor are made to pass through the calciner (RSTOIC reactor of Aspen Plus) where the calcination reaction process occurs:

2.3. Rotary kiln

The precalcining kiln is simulated as a series of linked RGIBBS Equilibrium reactor and YIELD blocks (reactor) with counter-current gas and solids flow in Fig. 2. Both the primary air and the kiln gas fuel were introduced at the kiln section, while the introduced combustion air was maintained 10% excess air and calcined raw meal enters the rotary kiln. First, the remaining $CaCO_3$ is converted to CaO in RGibbs reactor. A fraction of the solids as dust split out from the main solid stream and mixed with the rotary kiln flue gas. Kiln reactions simulated are $2CaO * SiO_2$, $3CaO * Al_2O_3$, and $3CaO * SiO_2$ and there are clinker components that are available in the Aspen Plus library. While ($4CaO * Al_2O_3 * Fe_2O_3$) is unavailable but represented with $CaO * Al_2O_3 * Fe$ was the fourth clinker component in the Aspen Plus library. Combustion in the main burner was simulated with RGibbs reactor.

2.4. Clinker cooler

The clinker cooler was simulated as a set of five heat exchangers in Fig. 2. Here, the clinker cooling air parameter was introduced to cool the clinker as well as provide combustion air for the rotary kiln. The first two heat exchangers heat secondary and tertiary air to 1050 °C and 704 °C, respectively, while the last three heat-exchanger cools the clinker to 105 °C and the heat recuperated is used for the drying of raw meal in a vertical roller mill. Before each heat exchanger, a part of the solid split out from the main stream as recuperated hot gas rotary kiln operation while the noodle-like clinker; combination of these four components ($2CaO * SiO_2$, $3CaO * Al_2O_3$, $CaO * Al_2O_3 * Fe$ and $3CaO * SiO_2$) as finished products.

3. Method and theoretical analysis

3.1. Thermodynamics balance equations

For a steady-flow process to find work, heat interactions, and energy efficiency, the following equations are applied to steady-state.

Mass balance

Eq. (1) represent mass balance of the system, which is expressed below

$$\Sigma \dot{m}_{in} = \Sigma \dot{m}_{out} \tag{1}$$

Bejan [35], expressed $\dot{m}$ as the mass flow rate, while the subscript 'in' is inlet and 'out' for outlet.

Energy balance

Energy balance equations can be expressed as Eq. (2) and (3) respectively.

$$\Sigma E_{in} = \Sigma E_{out} \tag{2}$$

$$Q_{netin} + \Sigma \dot{m}_{in} h_{in} = W_{netin} + \Sigma \dot{m}_{out} h_{out} \tag{3}$$

The rate of (energy transfer in) is represented as E_{in} while the rate of (energy transfer out) is E_{out} The rate of (net heat input) is expressed as; $Q_{netin} = Q_{in} - Q_{out}$, while the rate of (net work output) is represented as; $W_{netin} = W_{out} - W_{in}$, and the specific enthalpy is h. The energy balance expressed in Eq. (2) can further be simplified to enthalpy flow only, assuming constant kinetic and potential energies represented as Eq. (4):

$$\Sigma \dot{m}_{in} h_{in} = \Sigma \dot{m}_{out} h_{out} \tag{4}$$

A summary of an energy balance around the rotary kiln and grate cooler is given as Eq. (5) and (6)

$$\sum E_{in} = E_{kilnfeed} + E_{calcinerfuel} + E_{clinkercoolingair} + E_{kilnfuel} \tag{5}$$

$$\sum E_{out} = E_{coolerexhaustair} + E_{preheaterexitair} + E_{clinkerexit} \tag{6}$$

The system's efficiency equation is defined as Eq. (7)

$$\eta = \frac{\Sigma \dot{E}out}{\Sigma \dot{E}in} \tag{7}$$

3.2. Process simulation of the cement rotary kiln

Table 1 shows the input parameters used for simulation in Aspen Plus. Based on the data simulated in Aspen Plus, energy analysis of the streams was performed at the steady-state using Eqs. (1), (2), and (4). Cement rotary kiln energy efficiency was calculated using Eq. (7). In Aspen Plus, each stream was created with temperature, pressure, enthalpy, and internal energy. The energy of each stream was captured using the Aspen Plus process simulator at the fundamental operational conditions as well as at the reference states. Maximum energy was measured for both inlet and outlet of the network using Eq. (5) and (6), while Eq. (7) was used for estimating energy efficiency.

3.3. Artificial neural network modeling

An artificial neural network (ANN) was used to model the energy efficiency and product composition of the precalcining rotary kiln in a cement plant. The input data are presented through the input layer neurons and the corresponding results. The thirty (30) days of steady operational data (856 data) from the cement plants was used as input data for the Aspen plus to

Table 1 Input parameters for the simulation.

Rotary kiln properties	Operational data	Units
Kiln feed	205,000	kg/h
Kiln primary air fan	8500	kg/h
Gas flow in calciner	59.72	%
Gas flow in kiln	40.28	%
Raw meal/clinker factor	1.58	–
Preheater exit gas temperature	385	°C
Oxygen in preheater exit gas	3.85	%
Operation capacity	125,000	kg/h
Cooler total length	72	M
Cooling fans/total airflow	5/252500	kg/h

evaluate energy efficiency. The energy efficiency output neural network model is defined using the expression in Eq. (8).

$$y = (x_1, x_2, x_3, x_4, x_5 \ldots . x_n) \tag{8}$$

where y is energy efficiency, x_1, x_2, x_3, x_4, and x_5 are kiln feed mass flowrate, kiln gas flowrate, calciner gas flowrate, clinker cooling air, and primary air flowrate respectively. ANN simulation parameters used in the learning and training are the backpropagation algorithm, five input layers, thirty hidden layers, and one output layer, as shown in Fig. 3.

3.3.1. Data collection and preprocessing

This study focused on a cement precalcined rotary kiln process located in Ewekoro, Nigeria, and the data collected includes input variables and output variables. The distributed control system database was sampled once every minute, and approximately one month of data was collected. Ewekoro cement plant's operational parameters for the year 2019 were analysed and obtained from its records. These operational parameters include fuel gas, calciner temperature, secondary air pressure, raw feed material, and damper opening for the fan. The measured field data will be affected by the disturbance, especially for the cement calcination process, which will see high noise due to the gas–solid reaction entailed. The collected data were screened in order to determine which operational parameters should be considered relevant and consistent in the development of ANN and BANN model. Data gaps were identified and missed data was interpolated using the selected data based on statistical analysis. As shown in Table 2, a set of operational parameters were selected that each included 856 monthly data points.

Simulations of the neural network used similar model inputs for product compositions. Single hidden layer feedforward neural networks from MATLAB 2007 (MathWorks Inc., Natick, USA) are used for modeling the efficiency of energy and composition of products. In order to train, test and validate the ANN and BANN models in this study, 70% experimental datasets were used as training data (train data), while 15 % each was for testing and validation data. The ANN model was trained to establish a mapping function relationship between a condition and the outcome, with a target error for the actual and expected output values. If the output layer result is in advance greater than the target value of a given error, ANN must retrace step by step the original route of this signal and change the weighted value between the different neurons. During the model training process, the hidden layer constantly adjusts the weights between numerous neuron nodes through a transfer function to reduce the error of the model until reaching the set value. The network on the test data that gives the lowest squared error sum (SSE) is perceived to have the right number of hidden neurons. Network preparation, due to the various sizes of network's input layers and output layers, validation and test data is scaled to a range [-1, 1]. Conversely, when applied to unknown data due to overfitting noise in the data, traditional neural networks may lack generalization capability [36].

Levenberg-Marquardt was the choice training algorithm compared to conjugate gradient and resilient backpropagation. The choice of algorithm was done with a view to produce better results and with faster training for the application under consideration. With Levenberg-Marquardt algorithm, the goal of faster training to reduce global error was achieved with adjustments to weights and biases.

3.4. Bootstrap artificial neural network modeling (BANN)

To enhance the ANN and to decrease the value of error during the simulation process, the simulation was conducted by using BANN data learning model output. There is a possibility that different neural network models will perform well in different regions of the input space even when they are based on the same data set. Therefore, combining neural networks could enhance predictions on the whole input space. A bootstrap aggregates neural network model consists of different neural networks that are developed to model the same relationship. From bootstrap resampling replications of the original training data, an individual neural network models are developed. To improve model accuracy and robustness, several neural net-

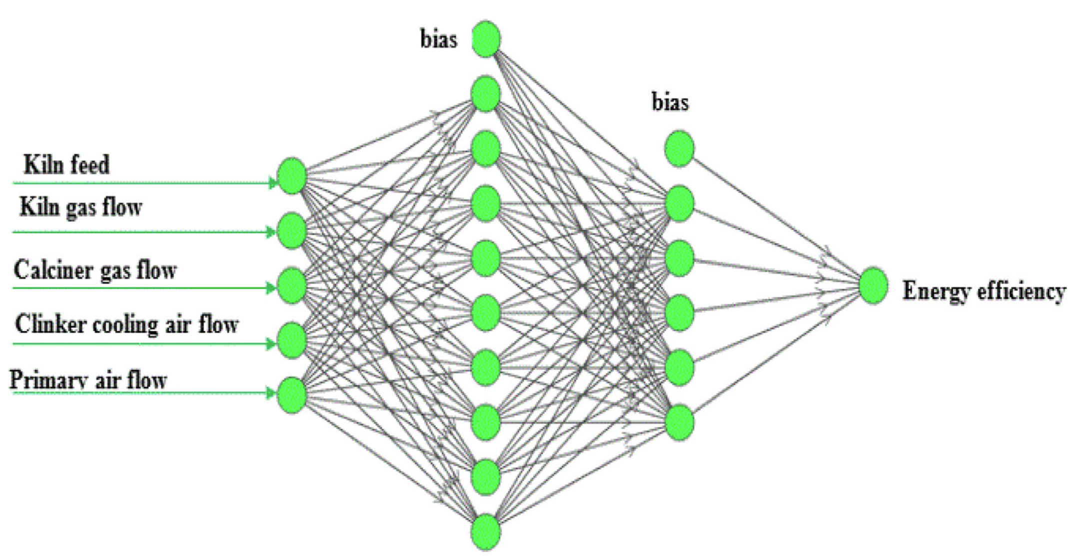

Fig. 3 The ANN architectures are used as a predictive model for energy efficiency.

Table 2 Plant operating parameters that are used in the development of ANN and BANN model.

Unit	Parameter	No. of data	Mean	Maximum	Minimum	SD	Mode
Precalcining rotary kiln	Kiln feed mass flowrate (kg/hr)	856	205,002	210,000	200,000	3739	206,700
	Kiln gas flowrate (kg/hr)	856	2821	3500	2000	543	3500
	Calciner gas flowrate (kg/hr)	856	5648	6500	4500	700	6500
	Clinker cooling air (kg/hr)	856	247,263	255,000	240,000	5598	240,000
	Primary air flowrate (kg/hr)	856	7296	8500	6000	934	8500
	Energy efficiency (%)	856	61.3	67.0	55	2.3	*NA

* NA: Not Applicable

works are combined instead of choosing one that is considered to be the best. These models can be developed on different parts of the data set. The bootstrap aggregated neural network can also be used to calculate model prediction confidence bounds from individual network predictions [Zhang J, 1999]. A diagram of a bootstrap aggregated neural network is shown in Fig. 4. A bootstrap aggregated neural network can be represented mathematically in Eq. (9)

$$f(X) = \sum_{i=1}^{n} w_i f_i(X) \tag{9}$$

where $f(X)$ is the aggregated neural network predictor, $f_i(X)$ is the *ith* neural network, w_i is the aggregating weight for combining the *ith* predicted neural network, n is the number of neural networks and X is a vector of neural network inputs. The overall output of bootstrap aggregated network is a combination of the weighted individual neural network output.

An assessment of the developed mathematical models: The statistical indices used in evaluating the neural networks model are defined in Eqs.(10) - (12):

$$R^2 = 1 - \sum_{i=1}^{n} \frac{(y_i - y_{di})^2}{(y_{di} - y_m)^2} \tag{10}$$

$$MSE = \frac{1}{n}\sum_{i=1}^{n} (y_i - y_{di})^2 \tag{11}$$

$$SSE = \sum_{i=1}^{n} (y_i - y_{di})^2 \tag{12}$$

$$AARE = \frac{1}{n}\sum_{i=1}^{n} \left[\frac{y_i - y_{di}}{y_{di}}\right] \tag{13}$$

R^2; coefficient of determination; MSE; mean square error; SSE: the sum of square error and absolute average relative error (AARE). Where n is the number of points, y_i is the predicted value obtained from the neural network model and Aspen Plus simulator, y_{di} is the experimental value, and y_m is the average of the experimental values.

4. Results and discussion

4.1. Process simulator using Aspen plus

Selected operational data from consistent steady running conditions of the cement plant were equated with simulation results to validate the process simulator. This includes the

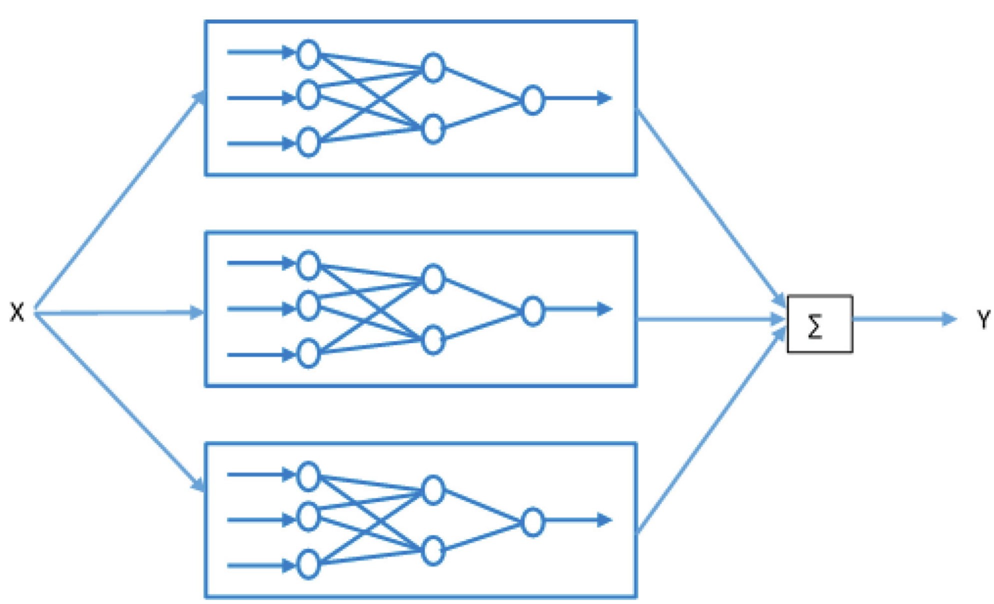

Fig. 4 A bootstrap aggregated neural network.

physical and chemical properties of each stream from the developed thermodynamic data. The validation results were summarized in Table 2. There is a slight deviation between the operational data and simulation results, which falls in the range of an acceptable limit of ± 2%. Although this does not in any way affect the result of the energetic efficiency of the plant studied. The results of the process simulator validation suggest that the process simulator is in good agreement and could be useful in predicting plant performance with an operating parameter of different sets.

The process simulator was further conducted using reference plant data to identify an area of improvement of the cement rotary kiln plant's energy performance. The mass and energy balance of the rotary kiln process is shown in Table 3, which provides the data for both inlet and outlet streams of the rotary kiln network. The energy efficiency for the cement rotary kiln system as indicated in Table 3 is 61.3%. The percentage of energetic efficiency obtained in this study was of the same trend with an estimated range of 60–70 % [4]. Based on the results presented on the Aspen Plus process simulator (Table 3), it was discovered that the Preheater / Calciner unit is linked with a high energy loss or dissipation. This mainly was due to decarbonation (calcination) taking place during the production process. Calcination, which is a chemical reaction is a significant source of thermodynamic inefficiency.

4.2. Artificial neural network (ANN) models

ANN models were used to estimate energy efficiency. ANN's performance depends on the method used in training the data sets, network structure, and results obtained at minimal error. Fig. 5 display the mean square error (MSE) for the training, testing, and validation data sets of the individual networks for energy efficiency. Table 5 expresses the model performance indicators for ANN and process simulator energy efficiency. The Sum of square Error (SSE) on the data sets training, testing, and unseen data (validation) are given in Table 4. Model performance indicators for ANN models achieved a mean square error (MSE) of 3.77×10^{-5} and 4.628×10^{-5} for the training and validation respectively. While the R^2 gives 0.991 and 0.984 for both the training and validation respectively. The sum of square error (SSE) is estimated as 0.0084 and 0.0091 for both the training and validation respectively. The produced model was validated using a set data for another 5 operating days that were not used in the training of the original model. The inference from this predictor shows that the model has a tendency to be used easily at various operating conditions to assess the energy efficiency of the rotary kiln process considering the error achieved compared to the Aspen Plus simulated value. Usually, the mass, enthalpies, and internal energy, of all the streams involved have to be generated by Aspen Plus in evaluating the energy efficiency while ANN brings an improvement since it does not involve the rigors of measuring stream mass, enthalpies, and internal energy.

4.3. Aggregated neural network in bootstrap

The energy efficiency of each system was modeled, a bootstrap aggregated neural network (BANN) that contains 30 neural networks was created. Every single network has one layer con-

Table 3 Material streams, operational and simulation data of process simulator validation.

Materials	Unit	Operational data	Simulated data	*AARE*
Main stream				
Kiln output	kg/h	125,000	125,500	0.004
Raw meal	kg/h	213,000	217,000	0.0184
Percentage of fuel in calciners	%	59.72	63.07	0.056
Percentage of fuel in kiln	%	40.28	36.93	0.083
Preheater exit gas dust	%	8.3	7.3	0.12
Raw meal/clinker factor	%	1.58	1.62	0.025
Gas stream				
Specific blowing density	Nm^3/kg clinker	2.2	2.1	0.045
Kiln inlet oxygen gas	%	2.8	2.08	0.26
Preheater exit oxygen gas	%	3.9	4.2	0.077
Heat stream				
Preheater exit gas temperature	°C	364	398	0.093
Clinker outlet temperature from kiln	°C	1350	1380	0.022
Secondary air temperature	°C	1050	1080	0.029
Tertiary air temperature	°C	902	854	0.053
Cooler exhaust air temperature	°C	275	302	0.098
Clinker cooler exit temperature	°C	110	105	0.045
Cooling efficiency	%	95	95.7	0.007
Chemical composition of clinker				
Tricalcium silicate ($3CaO{\bullet}SiO_2$)	wt%	61.1	62.2	0018
Dicalcium silicate ($2CaO{\bullet}SiO_2$)	wt%	16.6	18.4	0.110
Tetra-calcium aluminoferrite ($4CaOAl_2O_3Fe_2O_3$)	wt%	9.5	8.3	0.126
Tricalcium aluminate ($3CaO{\bullet}Al_2O_3$)	wt%	8.0	6.0	0.250

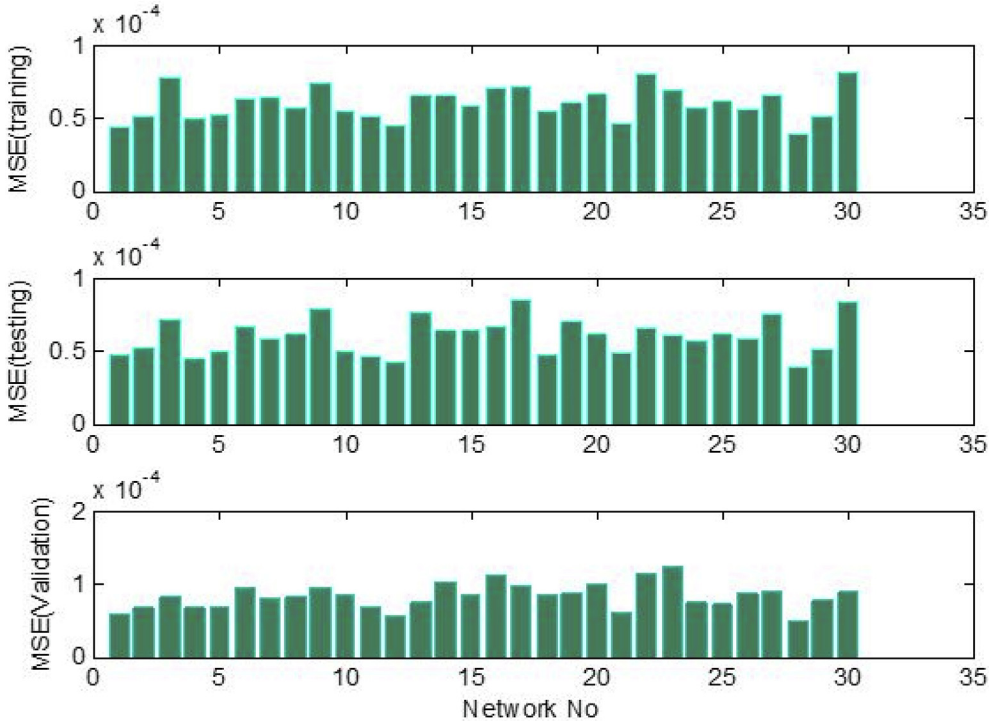

Fig. 5 Model errors of individual networks for energy efficiency of cement rotary kiln.

Table 4 Simulated data for energy analysis of a cement rotary kiln.

Equipment/ N° of input stream	Mass (kg/kg Cl)	Energy (kJ/kg)	Equipment/ N° of output stream	Mass (kg/kgCl)	Energy(kJ/kg)
Feed (108)	1.68	1549.49	Cooler clinker exit (67)	1.0	1263.97
Calciner fuel (3) & Calciner primary air (1)	0.42	722.83			329
Kiln fuel (43) & Kiln primary air (45)	0.10	6743.17	Preheater exit (13)	2.3	148.9
Cooling fans (34, 58, 60, 63, 68)	2.10	82.3	Cooler exhaust (73)	0.99	115.1
Total	4.30	3029	Total	4.30	1857
Energy Efficiency 61.3%					

Cl-clinker; N°-Number; 1, 3,13,34,43,45,58,60,63,67,68 73, and 108 are denoted in Fig. 2. process flow sheet.

cealed in it. The simulation algorithm Levenberg-Marquardt had been used to train the networks. Training data vary for each network. Several non-perfect models combined increase the prediction accuracy of the entire input space. For the rotary kiln process, the actual values obtained with the predicted from Bootstrap aggregated neural network (BANN) model efficiency for the training, testing and validation is shown in Fig. 6. Fig. 7 shows the MSE values for aggregated neural networks with different numbers of steady network, while the efficiency of individual networks on various data sets may be seen as inconsistent. A network with low MSE on the training data can have a wide MSE on validation information, which is an indication of non-robust for a single neural network [37]. The MSE for BANN models on training and testing data sets for the rotary kiln system energy efficiency is 3.64×10^{-5} and 5.00×10^{-5} respectively, this is an improvement

Table 5 Model performance indicators for ANN and process simulator (Aspen Plus) energy efficiency.

Model indicators	Training Set	Testing Set	Validation Set	Energy efficiency (%)	
SSE	0.00840	0.00540	0.00910	Process simulator	61.3
MSE	3.77×10^{-4}	3.94×10^{-4}	4.63×10^{-4}	ANN Model	61.5
R^2	0.991	0.990	0.984		

SSE: Sum of square error; MSE: Mean square error; R^2: Coefficient of determination

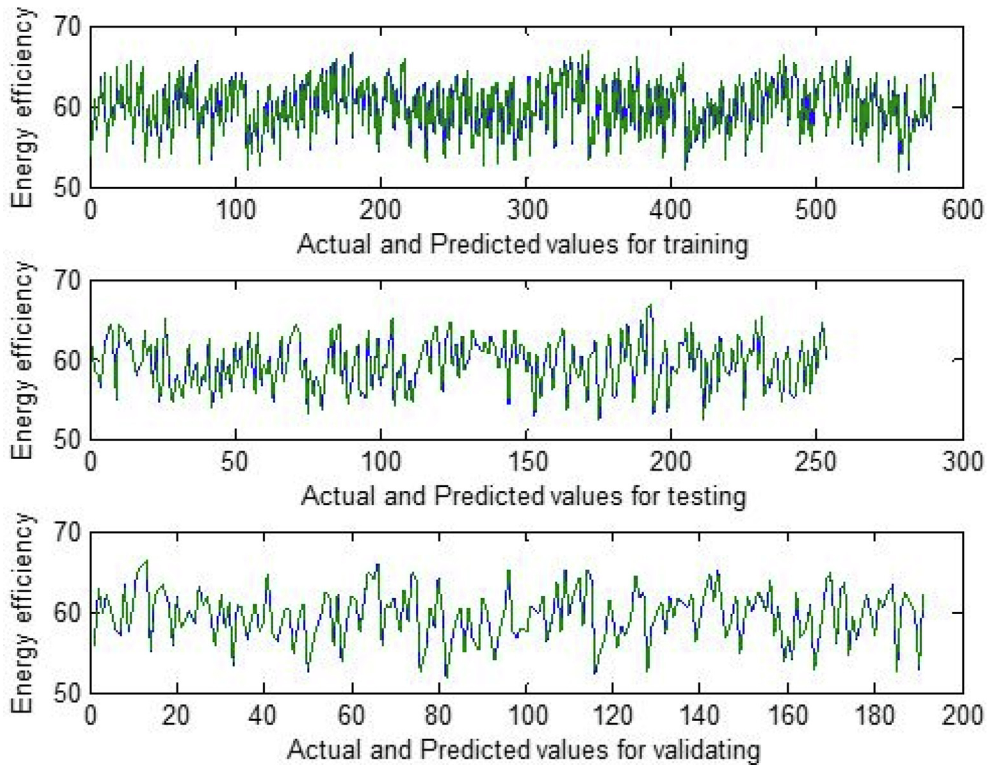

Fig. 6 Actual and BANN model predicted energy efficiency for the cement rotary kiln.

on the minimum MSE set in Table 4 for the single neural networks of ANN model. Fig. 8 shows the predicted and actual values of the energy efficiency as well as the confidence bounds. The prediction error lies between −0.024 and 0.025 as shown in Fig. 9. An advantage of BANN model is that it can offer model prediction confidence bound. A narrower confidence bound indicates that the associated model prediction is more reliable. Fig. 10. shows the plot between the predicted and actual energy efficiency of the cement rotary kiln production process. The accuracy of the model is shown to be enhanced with the use of an aggregated neural network model in bootstrap.

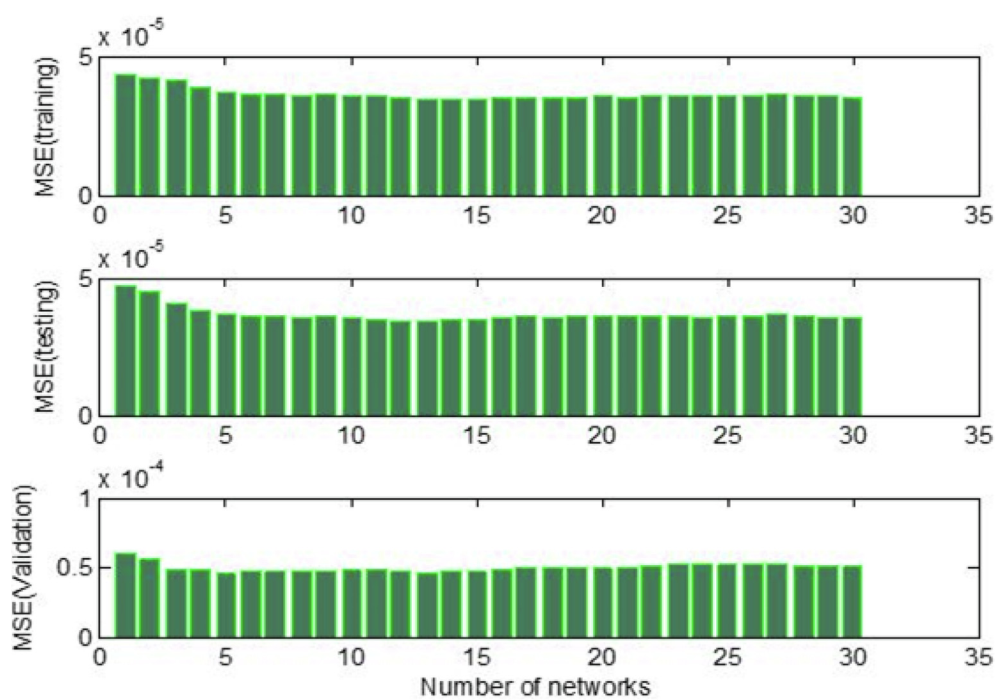

Fig. 7 Model errors of aggregated networks for energy efficiency of cement rotary kiln.

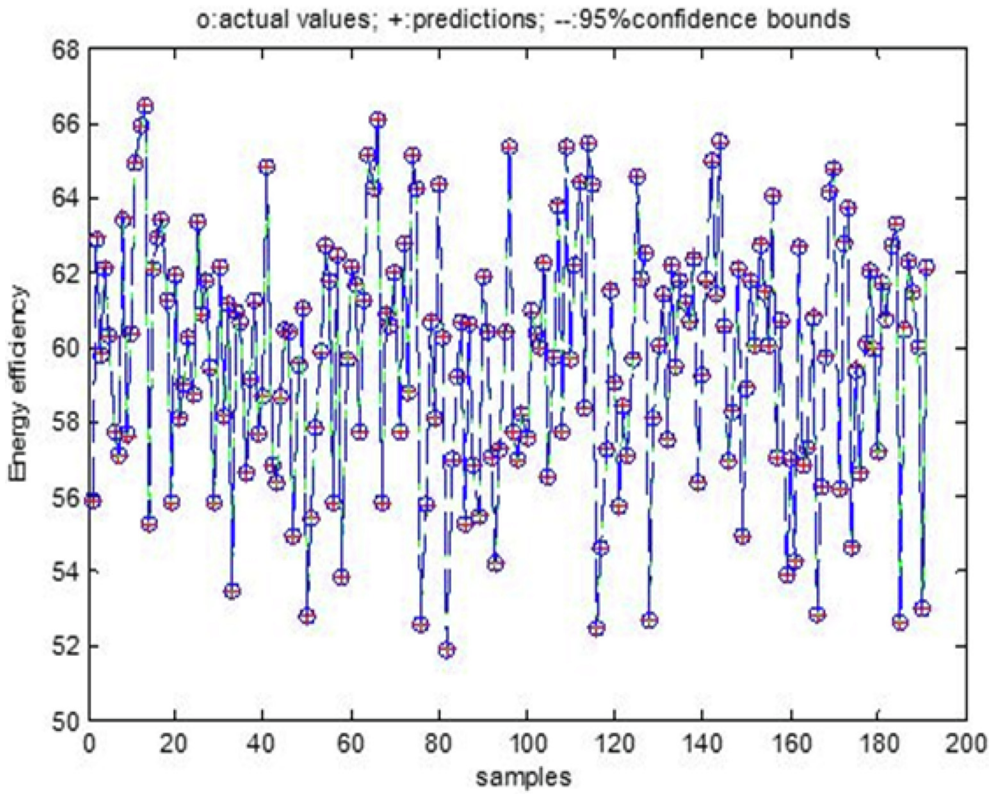

Fig. 8 The predicted and actual values of the energy efficiency as well as the confidence bounds.

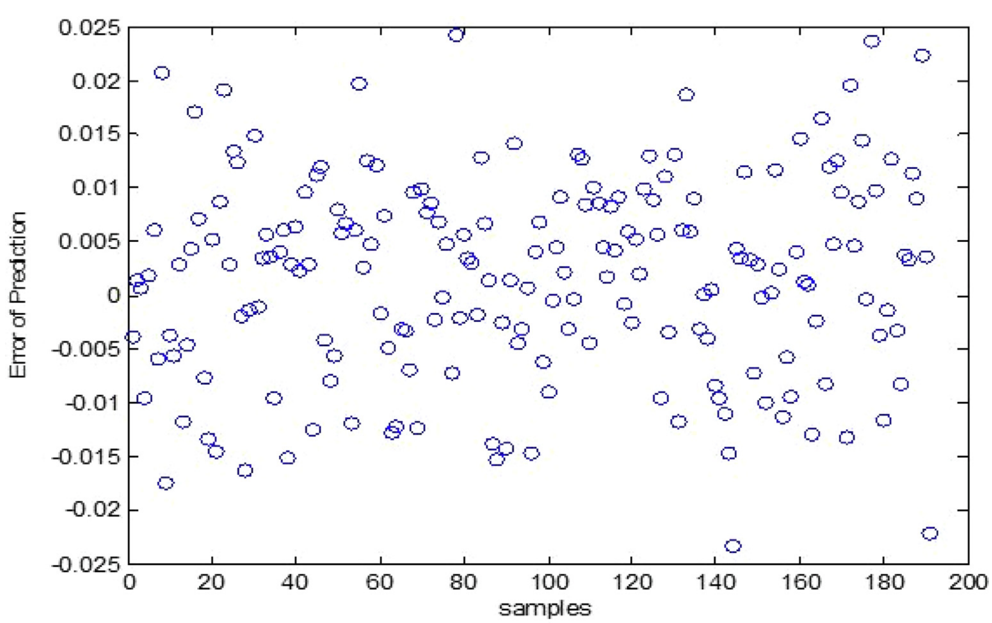

Fig. 9 Predictions and confidence bound of energy efficiency for cement rotary kiln BANN model.

4.4. Parametric study of precalcining rotary kiln

Maintaining a good energy efficiency is dependent on some of the operation parameters for the precalcining cement rotary kiln. Consequently, operation parameters such as kiln feed mass flowrate, kiln gas flowrate, calciner gas flowrate, clinker cooling air, and primary air flowrate were considered. Further, increasing and decreasing the kiln feed mass flow rate respectively would cause a change in energy efficiency of the cement rotary kiln system. A rise of 5 % above the optimal value in

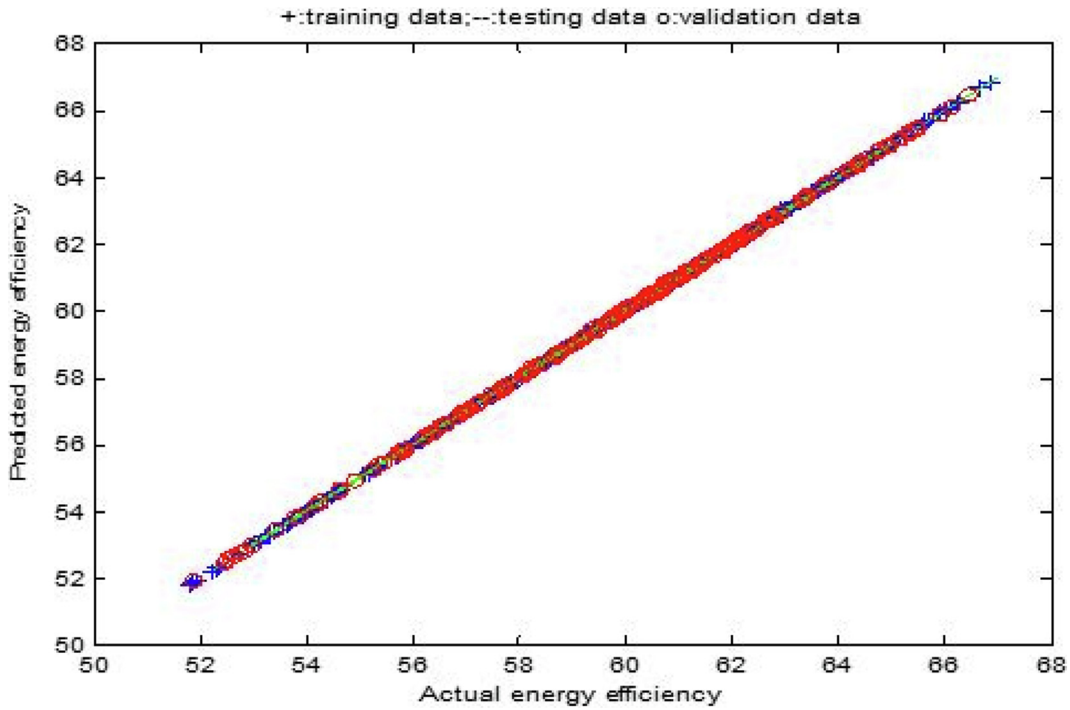

Fig. 10 Predicted and actual energy efficiency for cement rotary kiln BANN model.

the kiln feed mass flow rate with constant maximum calciner gas mass flow rate, would produce a rise in 1.2 % energy performance. Consequently, an increase of the primary airflow rate, leads to excess combustion air, which in turn cools down the temperature meant for calcination and clinker reaction processes. This corresponds to a 1.5 % reduction of energy performance. With a constant primary air flow rate in the calciner, a 5 % rise above the optimal value of calciner gas flow will increase the calciner temperature, which is equivalent to a 1.4 % rise in energy performance. However, a continuous rise in the gas causes the calciner's temperature to cool down due to incomplete combustion in the calciner. To compensate for the loss of primary air for calcination, an increase in primary air will be required in the calciner vessel to aid in complete combustion. Consequently, this would lead to operation instability and a loss of kiln operation resulting in poor clinker quality (off-spec). An attempt at operating the precalcining rotary kiln above the optimal parameters will be with a cost in terms of instability, and ultimately affect the quality of the product.

5. Conclusion

This paper uses BANN to improve non-linear models' robustness of individual artificial neural network. Consequently, the optimal operation parameters established for the precalcining rotary kiln using ANN were raw feed material of 205050 kg/hr, kiln fuel gas of 2821 kg/hr, calciner fuel gas of 5648 kg/hr, clinker cooling air of 247463 kg/hr and primary air of 7309 kg/hr at optimum predicted energy efficiency of 61.5 %. The operation parameters were validated experimentally using the Aspen process simulator and confirm through the plant process audit. Several sets of neural network training data can be created via bootstrap sampling when neural network models are being built. Using this technique, robustness of neural network models can be significantly improved. A further benefit of developing multiple neural networks based on bootstrap re-sampled data sets is that confidence bounds for neural network model predictions can be calculated. The energetic efficiency predicted by the use of BANN model with an estimated MSE of 3.64×10^{-5}, $3.70 \times 10^{-5,}$ and 5.00×10^{-5} for training, testing, and validation data sets, respectively. The studies on energy efficiency become a useful resource for investors, process design engineers, and plant operators in the assessment of the operating conditions on the rotary kiln of a cement plant.

CRediT authorship contribution statement

Anthony I. Okoji: Conceptualization, Writing – original draft. **Ambrose N. Anozie:** Conceptualization, Supervision, Writing – review & editing. **James A. Omoleye:** Supervision. **Abiola E. Taiwo:** Writing – review & editing. **Funmilayo N. Osuolale:** .

Declaration of Competing Interest

The authors declare that they have no known competing financial interests or personal relationships that could have appeared to influence the work reported in this paper.

Acknowledgments

The authors would like to acknowledge the Process and Simulation Laboratory of Landmark University for providing a suitable environment to carry out this research.

References

[1] Lafarge Africa. https://www.lafarge.com.ng/ 2019.
[2] Worrell E., Reuter M. Handbook of Recycling: State-of-the-art for Practitioners, Analysts, and Scientists: Newnes; 2014.
[3] Zafer Utlu, Ziya Sogut, Arif Hepbasli, Zuhal Oktay, Energy and exergy analyses of a raw mill in a cement production, Appl. Therm. Eng. 26 (17-18) (2006) 2479–2489.
[4] S. Fellaou, T. Bounahmidi, Evaluation of energy efficiency opportunities of a typical Moroccan cement plant: Part I. Energy analysis, Appl. Therm. Eng. 115 (2017) 1161–1172.
[5] Yousef S.H. Najjar, Douglas Waite, Energy conservation and waste utilization in the cement industry serve the green technology and environment, Int. J. Sustain. Eng. 9 (1) (2016) 3–10.
[6] M. Gebreslassie, K. Gebrelibanos, S. Belay, Energy consumption and saving potential in cement factory: thermal energy auditing, AFRREV STECH Int. J. Sci. Technol.. 7 (2) (2018) 92–106.
[7] D. Ha, S. Choi, Efficient Energy Management for Pyro-processing of Solids-(1) Heat & Mass Balance and Evaluation, J. Korean Soc. Combust. 21 (1) (2016) 18–30.
[8] Adem Atmaca, Recep Yumrutaş, Analysis of the parameters affecting energy consumption of a rotary kiln in cement industry, Appl. Therm. Eng. 66 (1-2) (2014) 435–444.
[9] M.Z. Sogut, Z. Oktay, A. Hepbasli, Energetic and exergetic assessment of a trass mill process in a cement plant, Energy Convers. Manage. 50 (9) (2009) 2316–2323.
[10] Okay Altun, Energy and cement quality optimization of a cement grinding circuit, Adv. Powder Technol. 29 (7) (2018) 1713–1723.
[11] A. Mehrpanahi, M.R. Aligoodarz, M. Zandieh, Comparative Energy and Exergy Analysis for the Utilization of Alternative Fuels in the Cement Kiln, Environ. Energy Economic Res. 4 (1) (2020) 15–26.
[12] Alireza Talaei, David Pier, Aishwarya V. Iyer, Md Ahiduzzaman, Amit Kumar, Assessment of long-term energy efficiency improvement and greenhouse gas emissions mitigation options for the cement industry, Energy 170 (2019) 1051–1066.
[13] A.I. Okoji, D.E. Babatunde, A.N. Anozie, J.A. Omoleye, Thermodynamic Analysis of Raw Mill in Cement Industry Using Aspen Plus Simulator, MS&E 413 (1) (2018) 012048.
[14] C. Pieper, B. Liedmann, S. Wirtz, V. Scherer, N. Bodendiek, S. Schaefer, Interaction of the combustion of refuse derived fuel with the clinker bed in rotary cement kilns: A numerical study, Fuel 266 (2020) 117048, https://doi.org/10.1016/j.fuel.2020.117048.
[15] W.K. Hiromi Ariyaratne, Anjana Malagalage, Morten C. Melaaen, Lars-André Tokheim, CFD modelling of meat and bone meal combustion in a cement rotary kiln–Investigation of fuel particle size and fuel feeding position impacts, Chem. Eng. Sci. 123 (2015) 596–608.
[16] Kaustubh S. Mujumdar, K.V. Ganesh, Sarita B. Kulkarni, Vivek V. Ranade, Rotary Cement Kiln Simulator (RoCKS): Integrated modeling of pre-heater, calciner, kiln and clinker cooler, Chem. Eng. Sci. 62 (9) (2007) 2590–2607.
[17] Xiang Xiao, Ping Fang, Jian-Hang Huang, Zi-Jun Tang, Xiong-Bo Chen, Hai-Wen Wu, Chao-Ping Cen, Zhi-Xiong Tang, Mechanistic study on NO reduction by sludge reburning in a pilot scale cement precalciner with different CO2 concentrations, RSC Adv. 9 (40) (2019) 22863–22874.
[18] A. Rahman, M.G. Rasul, M. Khan, S.C. Sharma, Assessment of energy performance and emission control using alternative fuels in cement industry through a process model, Energies. 10 (12) (2017) 1996.
[19] F.N. Osuolale, J. Zhang, Energy efficient control and optimisation of distillation column using artificial neural network, Chem. Eng. 39 (2014).
[20] Ergun Uzlu, Murat Kankal, Adem Akpınar, Tayfun Dede, Estimates of energy consumption in Turkey using neural networks with the teaching–learning-based optimization algorithm, Energy 75 (2014) 295–303.
[21] Jie Zhang, Developing robust non-linear models through bootstrap aggregated neural networks, Neurocomputing 25 (1-3) (1999) 93–113.
[22] Eriola Betiku, Victoria O. Odude, Niyi B. Ishola, Ayorinde Bamimore, Ajiboye S. Osunleke, Adebisi A. Okeleye, Predictive capability evaluation of RSM, ANFIS and ANN: A case of reduction of high free fatty acid of palm kernel oil via esterification process, Energy Convers. Manage. 124 (2016) 219–230.
[23] Hongjun Lin, Qunyun Dai, Lili Zheng, Huachang Hong, Wenjing Deng, Fuyong Wu, Radial basis function artificial neural network able to accurately predict disinfection by-product levels in tap water: Taking haloacetic acids as a case study, Chemosphere 248 (2020) 125999, https://doi.org/10.1016/j.chemosphere.2020.125999.
[24] Huachang Hong, Zhiying Zhang, Aidi Guo, Liguo Shen, Hongjie Sun, Yan Liang, Fuyong Wu, Hongjun Lin, Radial basis function artificial neural network (RBF ANN) as well as the hybrid method of RBF ANN and grey relational analysis able to well predict trihalomethanes levels in tap water, J. Hydrol. 591 (2020) 125574, https://doi.org/10.1016/j.jhydrol.2020.125574.
[25] Yifeng Chen, Liguo Shen, Renjie Li, Xianchao Xu, Huachang Hong, Hongjun Lin, Jianrong Chen, Quantification of interfacial energies associated with membrane fouling in a membrane bioreactor by using BP and GRNN artificial neural networks, J. Colloid Interf. Sci. 565 (2020) 1–10.
[26] Ying Deng, Xiaoling Zhou, Jiao Shen, Ge Xiao, Huachang Hong, Hongjun Lin, Fuyong Wu, Bao-Qiang Liao, New methods based on back propagation (BP) and radial basis function (RBF) artificial neural networks (ANNs) for predicting the occurrence of haloketones in tap water, Sci. Total Environ. 772 (2021) 145534, https://doi.org/10.1016/j.scitotenv.2021.145534.
[27] Haider M., Pakshirajan K., Singh A., Chaudhry S. Artificial neural network-genetic algorithm approach to optimize media constituents for enhancing lipase production by a soil microorganism. Applied biochemistry and biotechnology. 2008;144(3):225-35.
[28] H. Abu Qdais, K. Bani Hani, N. Shatnawi, Modeling and optimization of biogas production from a waste digester using artificial neural network and genetic algorithm, Resour. Conserv. Recycl. 54 (6) (2010) 359–363.
[29] Yu Feng, Wenfang Zhang, Dezhi Sun, Liqiu Zhang, Ozone concentration forecast method based on genetic algorithm optimized back propagation neural networks and support vector machine data classification, Atmos. Environ. 45 (11) (2011) 1979–1985.
[30] F.N. Koumboulis, N.D. Kouvakas, Indirect adaptive neural control for precalcination in cement plants, Math. Comput. Simul 60 (3-5) (2002) 325–334.
[31] Emilio Marengo, Marco Bobba, Elisa Robotti, Maria Cristina Liparota, Modeling of the polluting emissions from a cement production plant by partial least-squares, principal component regression, and artificial neural networks, Environ. Sci. Technol. 40 (1) (2006) 272–280.
[32] Dasaratha V. Sridhar, Richard C. Seagrave, Eric B. Bartlett, Process modeling using stacked neural networks, AIChE J. 42 (9) (1996) 2529–2539.
[33] David H. Wolpert, Stacked generalization, Neural Networks 5 (2) (1992) 241–259.
[34] J. Zhang, E.B. Martin, A.J. Morris, C. Kiparissides, Inferential estimation of polymer quality using stacked neural networks, Comput. Chem. Eng. 21 (1997) S1025–S1030.

[35] Bejan A. Advanced engineering thermodynamics: John Wiley & Sons; 2016.

[36] G.Peter Zhang, B.Eddy Patuwo, Michael Y. Hu, A simulation study of artificial neural networks for nonlinear time-series forecasting, Comput. Oper. Res. 28 (4) (2001) 381–396.

[37] Zhu C., Zhang J., editors. Developing robust nonlinear models through bootstrap aggregated deep belief networks. 2019 25th International Conference on Automation and Computing (ICAC); 2019: IEEE.https://doi.org/10.23919/IConAC.2019.8895070